

# Packing of the Transmembrane Helices of Na,K-ATPase: Direct Contact between $\beta$ -Subunit and H8 Segment of $\alpha$ -Subunit Revealed by Oxidative Cross-Linking<sup>†</sup>

Alexander Ivanov, Hao Zhao, and Nikolai N. Modyanov\*

Department of Pharmacology, Medical College of Ohio, Toledo, Ohio 43614 USA

Received May 2, 2000

**ABSTRACT:** Spatial relationships among the transmembrane (TM) segments of  $\alpha$ - and  $\beta$ -subunits of the Na,K-ATPase molecule have been investigated using oxidative induction of disulfide bonds. The catalytic  $\alpha$ -subunit contains 10 TM  $\alpha$ -helices (H1–H10) with 9 Cys residues located within or close to the membrane moiety. There is one Cys residue in the single TM segment of  $\beta$ -subunit (H $\beta$ ). Previously, the cross-linking products containing the  $\beta$ -subunit and two fragments of  $\alpha$ -subunit (the N-terminal containing H1–H2 helices and the C-terminal containing H7–H10 helices) have been identified in experiments with membrane-bound or detergent-solubilized preparations of the membrane moiety of trypsin-digested Na,K-ATPase [Sarvazyan, N. A., Modyanov, N. N., and Askari, A. (1995) *J. Biol. Chem.* 270, 26528–26532 and Sarvazyan, N. A., Ivanov, A., Modyanov, N. N., and Askari, A. (1997) *J. Biol. Chem.* 272, 7855–7858]. Here, we have shown that Cu<sup>2+</sup>-phenanthroline treatment of digitonin-solubilized preparation provides the most efficient formation of intersubunit cross-linked product that is predominantly a dimer of  $\beta$ -subunit and a 22-kDa C-terminal  $\alpha$ -fragment containing H7–H10 helices. This cross-linked product was isolated and subjected to CNBr cleavage. The resulting fragments were electrophoretically separated and sequenced. A 17-kDa peptide composed of Ile853–Met942  $\alpha$ -fragment and Ala5–Met56  $\beta$ -fragment was identified as a product of intersubunit disulfide cross-link between Cys44 of H $\beta$  and either Cys911 or Cys930, located in H8. This provides the first direct experimental evidence of the juxtaposition of H $\beta$  and H8 within the Na,K-ATPase molecule. The second detected cross-linked product was composed of  $\alpha$ -fragments Lys947–Met963 and Tyr974–Tyr1016 linked by induced disulfide bridge between Cys964 (H9) and Cys983 (H10). The spatial proximity of these Cys residues defines the mutual orientation of H9 and H10 helices of  $\alpha$ -subunit.

Na,K-ATPase,<sup>1</sup> a P-type ATPase, is a ubiquitous ion pump responsible for coupled active transport of Na<sup>+</sup> and K<sup>+</sup> across the cell membrane (1, 2). This enzyme belongs to the X,K-ATPase subfamily that also includes closely related gastric and nongastric H,K-ATPases. Like other X,K-ATPases, the Na,K-ATPase consists of two subunits,  $\alpha$  and  $\beta$ , associated in an equimolar ratio. (The renal enzyme contains also a third component,  $\gamma$ -subunit, of ~6.5 kDa.) The catalytic  $\alpha$ -subunit (~112 kDa), a polytopic protein with 10 TM segments (H1–H10), contains the ATP-hydrolyzing center on the large cytoplasmic protrusion, cation binding and occlusion sites within the membrane, and receptor for cardiac glycosides on the extracellular surface. The  $\beta$ -subunit (~35 kDa), a glycoprotein with a single TM segment (H $\beta$ ), plays a major role in formation of the mature functionally active  $\alpha\beta$

complex and its targeting to plasma membrane and also influences the holoenzyme's enzymatic and transport functions. Other animal P-ATPases such as sarcoplasmic reticulum (SR) Ca-ATPase, for example, contain no subunits analogous to  $\beta$ -subunits of X,K-ATPases (1–4).

Although the Na,K-ATPase subunits are not linked by covalent bonds, intersubunit interactions are strong enough that the complex remains stable upon solubilization in nonionic detergents, and subunits can be separated only using SDS. Experimental data suggest that several protein regions located in extracellular, intramembrane, and cytoplasmic domains are involved in structurally and functionally essential interactions between  $\alpha$ - and  $\beta$ -subunits (5–13). Thus, in studies of chimeras between the Na,K-ATPase and Ca-ATPase (5), twenty-six extracellular residues from the loop connecting the H7 and H8 TM segments of  $\alpha$  and the highly conservative tetrapeptide SYGQ, in particular, have been implicated as providing the site for association with the  $\beta$ -ectodomain (5, 6). Several residues in this loop were identified as essential for  $\alpha$ – $\beta$  interaction in site-directed mutagenesis studies (11). The interactive part of the  $\beta$ -ectodomain was shown to be within 63 amino acids adjacent to the H $\beta$  TM segment by using the yeast two-hybrid system (6). Currently, these extracellular interactions are considered as a key step in  $\alpha\beta$  assembly (5, 6, 8–11). Other data also suggest that interaction of the TM domain

<sup>†</sup> This work was supported by National Institutes of Health Grants GM54997 and HL-36573.

\* To whom correspondence should be addressed at Department of Pharmacology, Medical College of Ohio, 3035 Arlington Avenue, Toledo, OH 43614-5804. Telephone: (419) 383-4182. Fax: (419) 383-2871. E-mail: nmodyanov@mco.edu.

<sup>1</sup> Abbreviations: PAGE, polyacrylamide gel electrophoresis; PVDF, poly(vinylidene difluoride); H, hydrophobic  $\alpha$ -helix forming transmembrane (TM) segment; Tricine, N-[2-hydroxy-1,1-bis(hydroxymethyl)ethyl]glycine; NEM, N-ethyl-maleimide; CPM, 7-diethylamino-3-(4'-maleimidylphenyl)-4-methylcoumarin; CAPS, 3-(cyclohexylamino)-1-propanesulfonic acid; TID, 3-(trifluoromethyl)-3-(meta-[<sup>125</sup>I]iodophenyl)-diazirine.

of the  $\beta$ -subunit is also important for efficient and stable assembly with the  $\alpha$ -subunit (12, 13).

The important aspects of spatial structure of the Na,K-ATPase membrane moiety, such as intramembrane arrangement of TM segments, are unknown, and the available experimental data are rather limited. Our earlier spectroscopic studies of the enzyme membrane moiety deprived of extra- and intracellular domains by trypsin cleavage have demonstrated predominantly  $\alpha$ -helical structure of TM segments (14, 15). These data combined with electron microscopic analysis of two-dimensional crystals (16), hydrophobic photolabeling, and prediction of helix orientation with respect to lipid (14, 17, 18) were used to calculate the first tentative models of helix packing within the Na,K-ATPase membrane moiety (19–22). Recently, a more detailed model of helix packing of related P-ATPase, SR Ca-ATPase, was proposed based on spatial structure solved at 8-Å resolution (23). However, in this model, the locations of particular TM segments relative to each other are still hypothetical except for the H4 and H6 TM helices whose direct contact was determined by sulfhydryl cross-linking (24). It should be mentioned that amino acid sequences of the Na,K-ATPase  $\alpha$ -subunit and Ca-ATPase exhibit significant levels of similarity in H4,H5–H6 segments, but not in the other TM segments. Therefore, the possibility cannot be excluded that TM segment packing in membrane moieties may be quite different and specific for each of these P-ATPases.

It was demonstrated in earlier studies of several laboratories that intersubunit  $\alpha,\beta$ -dimer is the major product of oxidative cross-linking of detergent-solubilized preparations of Na,K-ATPase catalyzed by  $\text{Cu}^{2+}$  or  $\text{Cu}^{2+}$ -phenanthroline complex (25–31). In subsequent studies on identification of contacts between intramembrane domains within Na,K-ATPase molecule, we applied the oxidative sulfhydryl cross-linking technique to the native and digitonin-solubilized preparations of the canine kidney enzyme subjected to different types of selective proteolysis (7, 32, 33). Analysis of isolated intramembrane cross-linked products indicated that the single TM helix of  $\beta$ -subunit is in direct contact with H8–H10 intramembrane domain of  $\alpha$ -subunit, and there is close intrasubunit contact between N-terminal (H1–H2) and C-terminal (H7–H10) fragments of  $\alpha$ -subunit (7, 32, 33). The results of further characterization of direct intramembrane helix–helix contacts presented in this report establish the juxtaposition of H $\beta$  and H8. It should be noted that after we had demonstrated through cross-linking studies that H $\beta$  is in contact with the TM helices of the  $\alpha$ -subunit (7, 32), Or et al. (34) confirmed this conclusion by similar studies and based on indirect evidence suggested that the H $\beta$  contact may be with the H8 of the  $\alpha$ -subunit. The present studies provide direct evidence for the existence of H $\beta$ –H8 interaction. A preliminary account of this work has been presented (35).

## EXPERIMENTAL PROCEDURES

The purified membrane-bound  $\text{Na}^+/\text{K}^+$ -ATPase of canine kidney medulla, with specific activity of 1000–1600  $\mu\text{mol}$  of ATP hydrolyzed ( $\text{mg}$  of protein) $^{-1}$   $\text{h}^{-1}$  was prepared and assayed as described before (7, 32, 33). The purified enzyme was stored in 250 mM sucrose, 30 mM histidine, 1 mM EDTA buffer solution, pH 6.8, at  $-70^\circ\text{C}$  until used. Up to

45 mg of this preparation has been used in a large-scale cross-linking experiment.

**Proteolytic Digestion.** Samples of the Na,K-ATPase membrane moiety were prepared by extensive trypsin treatment of purified enzyme as described previously (7, 32–34, 36). Briefly, initial preparations were suspended (0.5 mg/mL) in a solution containing 10 mM RbCl, 10 mM Tris-HCl (pH 8.5), and 1.5 mM EDTA and incubated at  $37^\circ\text{C}$  for 1 h with trypsin (0.2 mg/mg of Na,K-ATPase). Soybean trypsin inhibitor was added (5 mg/mg of trypsin) to stop the digestion, and samples were incubated an additional 5 min at  $37^\circ\text{C}$ . The membrane-bound fragments were collected by centrifugation and washed twice with 10 mM Tris-HCl (pH 7.4). Trypsin, type XIII from bovine pancreas, and the trypsin inhibitor were obtained from Sigma.

**Solubilization.** Preparation of the Na,K-ATPase membrane moiety was suspended (1.35 mg/mL) in 10 mM Tris-HCl (pH 7.4) and solubilized by mixing with an equal volume of 6 mg/mL digitonin, stirred for 5 min at  $24^\circ\text{C}$ , and centrifuged for 30 min at 100000g. The clear supernatant containing the solubilized membrane moiety was collected.

**Cross-Linking.** Oxidative cross-linking of the above digitonin solubilized preparation was as done as described before (7, 32, 33) by incubation for 15 min in a solution containing 0.25 mM  $\text{CuSO}_4$  and 1.25 mM *o*-phenanthroline (10 mM Tris-HCl, pH 7.4,  $24^\circ\text{C}$ ). These conditions were chosen after preliminary experiments using the approach described before (37). The reaction was terminated by the addition of EDTA to a final concentration of 30 mM, followed by incubation for 5 min at room temperature.

**Modification of Free Cys Residues.** Free SH-groups of Cys residues after cross-linking reaction were blocked by treatment with NEM at room temperature for 1 h in the presence of 0.5% SDS and 10 mM Tris-HCl (pH 7.4). Equal amounts of NEM were added with 30 min interval to a final concentration of 30 mM. The sample was then precipitated with 4 vol of methanol overnight at  $-20^\circ\text{C}$ . Membrane pellets were collected by centrifugation and washed with 10 mM Tris-HCl (pH 7.4). Usually about 5/6 of the cross-linked products were treated in this way. Free Cys residues in the rest of the sample were labeled with fluorescent CPM (Molecular Probes). Modification was performed in the presence of 0.1 mM CPM and 0.5% SDS for 1 h in the dark at room temperature.

**Isolation of Cross-Linked Products.** Pellets of NEM-treated cross-linked products were dissolved by sequential adding of equal volumes of 10 M urea, 10% SDS, and 125 mM Tris-HCl (pH 6.8) and combined with the CPM-labeled peptides. Cross-linked peptides were separated by electrophoresis on 10% Tricine/SDS polyacrylamide gels (38). For preparative purposes,  $180 \times 200 \times 1.5$  mm gels were run overnight at  $4^\circ\text{C}$  at constant voltage (110 V). Small gels ( $85 \times 75 \times 0.75$  mm) were run at constant voltage (60 V) for 4–5 h at room temperature. Sulfhydryl reagents were omitted from the buffers used for electrophoresis to preserve the cross-linked products. In case of preparative electrophoresis of CPM and NEM modified samples, bands of interest were detected under UV light, cut out from unfixed and unstained gels, and eluted with 50 mM ammonium bicarbonate containing 0.1% SDS and 10  $\mu\text{M}$  tryptophan, using Bio-Rad electroelution chamber overnight, 8 mA per

tube. Collected samples were lyophilized. Lyophilization was repeated twice.

**Treatment with N-Glycosidase F.** Lyophilized sample of cross-linked product "Bs" was dissolved in 50 mM sodium phosphate (pH 7.5) containing 1% NP-40 and 10  $\mu$ M tryptophan. Deglycosylation was performed with N-glycosidase F (PNGase F, New England BioLabs) for 24 h at room temperature. After this, the reaction mixture was diluted with water and lyophilized.

**CNBr Cleavage and Isolation of the Peptide Fragments.** Lyophilized samples of cross-linked product (before or after deglycosylation) were dissolved in 0.5 mL of 70% formic acid containing 10  $\mu$ M tryptophan and cleaved with CNBr (~300-fold molar excess over Met residues in the sample) under nitrogen for 20 h in the dark at room temperature. To remove excess acid, samples were diluted 10 times with water and lyophilized. Lyophilization was repeated twice. CNBr peptides were dissolved in 10 M urea/10% SDS/125 mM Tris-HCl, pH 6.8 (1:1:1), and separated by electrophoresis on 16.5% Tricine/SDS polyacrylamide gels (180  $\times$  200  $\times$  0.75 mm) at constant current (30 mA) for 25–30 h at 5  $^{\circ}$ C.

After electrophoresis was performed, peptide fragments from unstained gel were transferred to PVDF membrane by electroblotting in 10 mM CAPS and 10% methanol, pH 11, detected on the membrane by brief staining with 0.1% Coomassie brilliant blue R-250 in 50% methanol, destained by washing several times with 50% methanol, rinsed with water, and dried as described before (39). The peptide bands were excised from the PVDF membrane and subjected to N-terminal amino acid sequencing. Immunoblot analysis was performed as described previously (7).

## RESULTS AND DISCUSSION

**Isolation of Cross-Linked Product Composed of  $\beta$ -Subunit and a 22-kDa C-terminal  $\alpha$ -Fragment.** The main aim of this study was to determine which particular TM segment of the Na,K-ATPase  $\alpha$ -subunit contains the Cys residue forming intersubunit disulfide cross-link with Cys 44 of the single TM helix of the  $\beta$ -subunit. Cross-linking experiments with  $\text{Cu}^{2+}$ -phenanthroline described here were performed using samples of the Na,K-ATPase membrane moiety deprived of intracellular domains by extensive trypsin digestion according to established procedures (7, 32–34, 36) as described in Experimental Procedures. The resolution of the constituent peptide fragments of the membrane moiety on Tricine/SDS gels is shown in Figure 1, lane 1. Major components of this well-characterized preparation are four fragments of the  $\alpha$ -subunit, the large C-terminal 22-kDa fragment N831–Y1016 comprising H7–H10, and three smaller fragments containing membrane-spanning hairpins H1–H2 (11-kDa peptide, N-terminal N68), H3–H4 (9-kDa peptide, N-terminal I263), and H5–H6 (10-kDa peptide, Q737–R830), and the polypeptide chain of the  $\beta$ -subunit beginning at Ala5, part of which is cleaved at Arg142–Gly143 (7, 32–34, 36). This preparation also contains the  $\gamma$ -subunit (36, 40) and a number of minor components including the C-terminal 32-kDa fragment Q737–Y1016 (Modyanov et al., unpublished observations).

In agreement with previous results (32, 33), the incubation of this membrane-bound preparation with  $\text{Cu}^{2+}$ -phenanthroline results in the formation of two cross-linked products

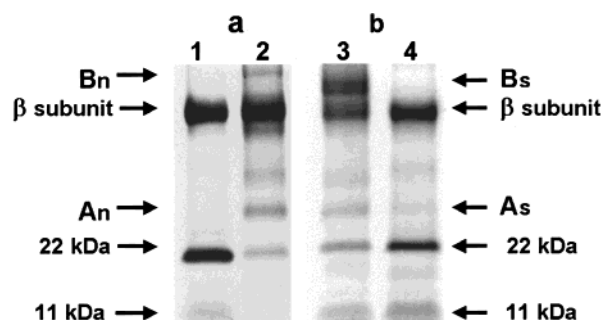


FIGURE 1:  $\text{Cu}^{2+}$ -phenanthroline induced oxidative cross-linking of the membrane-bound (a) and digitonin-solubilized (b) preparations of the Na,K-ATPase membrane moiety obtained after extensive trypsin digestion. Membrane samples were prepared, cross-linked, and resolved on 10% Tricine/SDS polyacrylamide gels as described in Experimental Procedures. (a) Membrane-bound preparation prior to cross-linking (lane 1) and after cross-linking (lane 2). (b) Digitonin-solubilized preparation before cross-linking (lane 4) and after cross-linking (lane 3). (See text for details.)

designated as "An" and "Bn" (Figure 1, lane 2). The product "An", which consists of N-terminal (11 kDa) and C-terminal (22 kDa) peptides of  $\alpha$ -subunit, is a predominant product of cross-linking reactions in these conditions. (Further structural study of the intrasubunit 11,22 cross-linked product will be presented elsewhere). Under these experimental conditions, however, the desired intersubunit cross-linked product "Bn" (Figure 1, lane 2), which is a trimer of  $\beta$ -subunit and two (11- and 22-kDa) fragments of  $\alpha$ -subunit designated as 11,22, $\beta$ -trimer, comprises only a minor portion of cross-linked products (32). Previously, we demonstrated that the trimer of  $\beta$ - and  $\alpha$ -fragments of 11- and 22-kDa formed with much higher yield upon  $\text{Cu}^{2+}$ -induced cross-linking of digitonin-solubilized preparation of Na,K-ATPase membrane moiety (7). Evidently, some backbone flexibility induced by detergent solubilization, is required for close juxtaposition of the Cys44 of  $\beta$  with one of the nearby intramembrane cysteines of  $\alpha$  to allow the disulfide bridge formation.

In the current study, the digitonin-solubilized preparation of Na,K-ATPase membrane moiety (Figure 1, lane 4) was cross-linked in the presence of  $\text{Cu}^{2+}$ -phenanthroline complex. The reaction mixture was treated with *N*-ethylmaleimide to block free SH-groups of Cys residues and resolved on 10% Tricine/SDS gel (Figure 1, lane 3). Under these experimental conditions, the formation of  $\alpha$ - $\beta$  intersubunit cross-links was very efficient and provides a high yield of the major product of cross-linking reactions with molecular mass of about 80 kDa, designated as "Bs" in Figure 1. In contrast, low molecular weight cross-linked product "As", which like product "An" (Figure 1, lane 2) consists of N-terminal (11 kDa) and C-terminal (22 kDa) peptides of  $\alpha$ -subunit (data not shown), formed only in trace amounts under these conditions, and therefore it was not further analyzed. The peptide composition of the cross-linked product "Bs" was determined by N-terminal sequencing (Table 1).

As shown in Table 1, the N-terminal sequences corresponding to the 22-kDa C-terminal  $\alpha$ -fragment beginning at Asn831 and the truncated  $\beta$ -subunit polypeptide chain starting from Ala5 were present in an equimolar ratio. The approximate yield of these sequences was about five times higher than that of the sequence corresponding to the N-terminal 11-kDa  $\alpha$ -fragment, which starts at Asp68. The second sequence derived from the  $\beta$ -subunit starts at Gly143.

Table 1: N-terminal Sequence Analysis of the Cross-Linked Product Bs<sup>a</sup>

sequence	polypeptide chain region	yield pmol
<sup>831</sup> Asn-Pro-Lys-The-Asp-Lys-Leu-Val	$\alpha$ -subunit, C-terminal domain (H7-H10)	35
<sup>5</sup> Ala-Lys-Glu-Glu-Gly-Ser-Xaa-Lys	$\beta$ -subunit, truncated at N-terminus	37
<sup>143</sup> Gly-Glu-Arg-Lys-Val-Xaa-Arg-Phe	$\beta$ -subunit, C-terminal half	17
<sup>68</sup> Asp-Gly-Pro-Asn-Ala-Leu-Thr-Pro	$\alpha$ -subunit, H1-H2	6

<sup>a</sup> Cross-linked product designated as "Bs" in Figure 1, lane 3 was analyzed as indicated in Experimental Procedures. The sequences were followed for eight cycles of Edman degradation and were identical with shown fragments of the dog kidney Na,K-ATPase  $\alpha_1$  and  $\beta_1$  subunits (41, 42). Xaa's indicate amino acid residues that were not identified upon sequencing and correspond to Cyl48 of  $\alpha$ -subunit and Trp11 of  $\beta$ -subunit. The approximate yield of each sequence was estimated from the average elevation of amino acid residues in cycles 2 through 8.

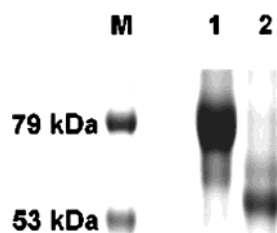


FIGURE 2: Electrophoretic analysis of isolated intersubunit cross-linked product "Bs" before (lane 1) and after (lane 2) deglycosylation on 10% Tricine/SDS polyacrylamide gel. Treatment with N-glycosidase F was done as described in Experimental Procedures. The amount of sample in lane 1 was about three times larger than loading of deglycosylated sample in lane 2. M, molecular mass markers.

Its presence indicated that a significant portion (about 50%) of the cross-linked  $\beta$  is also cleaved at Arg142-Gly143. The N- and C-terminal parts of this cleaved  $\beta$ -chain remain connected by an endogenous disulfide bridge Cys125-Cys148. Considered together, the data of Table 1 demonstrate that the isolated intersubunit cross-linked product consists predominantly of a dimer of the 22-kDa C-terminal  $\alpha$ -fragment and the  $\beta$ -subunit polypeptide, partially cleaved at Arg142-Gly143. Relatively low yield of the sequence of 11-kDa  $\alpha$ -fragment indicates that the 11,22, $\beta$ -trimer comprises only a minor fraction of the intersubunit cross-linked product.

Thus, cross-linking reactions of digitonin-solubilized preparation of Na,K-ATPase membrane moiety catalyzed by Cu<sup>2+</sup>-phenanthroline complex lead to the predominant formation of the cross-linked 22, $\beta$ -dimer, whereas Cu<sup>2+</sup> catalyzes the formation of the 11,22, $\beta$ -trimer under these conditions (7). This difference most probably indicates that the Cu<sup>2+</sup> ion has a higher ability to penetrate in close proximity to Cys residues involved in formation of cross-link between 11- and 22-kDa  $\alpha$ -fragments than the Cu<sup>2+</sup>-phenanthroline complex. Because of more simple composition, the 22, $\beta$ -dimer has an obvious advantage with respect to structural analysis directed to the identification of intersubunit contacts.

It should be noted that due to the presence of the carbohydrate moiety in the  $\beta$ -subunit, both products of intersubunit cross-linking reactions, 22, $\beta$ -dimer and 11,22, $\beta$ -trimer, migrate as one broad band upon electrophoresis in 10% Tricine/SDS gel (Figure 2, lane 1). As shown in Figure 2, lane 2, treatment with N-glycosidase F allowed the separation of the components of the cross-linked product "Bs". After deglycosylation, the main cross-linked product migrates as 56-kDa protein. This correlates well with the expected molecular mass of the protein moiety of the 22, $\beta$ -dimer. A barely detectable upper band of about 63 kDa represents the minor cross-linked product 11,22, $\beta$ -trimer.

Several large scale experiments were performed to isolate the intersubunit cross-linked product in amounts sufficient for further structural analysis. To avoid fixation of preparative gels and their staining with Coomassie, a small fraction of the products of the cross-linking reactions were treated with a fluorescent CPM, instead of NEM, before loading on polyacrylamide gels. After electrophoresis, the bands of interest were detected under UV light, excised from unfixed and unstained gels, electroeluted, and lyophilized.

*Structural Analysis of Peptide Fragments Obtained after CNBr Cleavage of the 22, $\beta$ -Dimer.* An optimal procedure for further fragmentation of isolated cross-linked product and separation of resulting peptides was developed in preliminary experiments. Analytical experiments on tryptic digestion resulted in a complex mixture of peptides, most of which were products of incomplete cleavage. Attempts to isolate individual tryptic peptides containing intersubunit cross-links were unsuccessful. Much better resolution of resulting peptide fragments was obtained by CNBr cleavage. This experimental approach has a potential problem. To preserve the integrity of the cross-linked products, reducing sulfhydryl reagents must be omitted from the buffers used for electrophoresis and other experiments. This in turn increases a probability of Met oxidation to sulfone or sulfoxide, whose peptide bonds cannot be cleaved by CNBr. To overcome this potential problem, we used buffers containing 10  $\mu$ M tryptophan as a trap for oxidizing agents. Cyanogen bromide cleavage of the isolated intersubunit cross-linked product "Bs" (Figure 1, lane 3 and Figure 2, lane 1) was performed as described in Experimental Procedures.

A schematic map of intersubunit cross-linked product structure is shown in Figure 3. There are four Cys residues in the 22-kDa fragment that may form a cross-link with Cys44 of H $\beta$ : Cys911 and Cys930 (H8), Cys964 (H9), and Cys983 (H10). Taking into account all possible combinations, the expected molecular mass of the intersubunit cross-linked product after CNBr cleavage may be estimated to be either 9.3 or 11.9 or 17.1 kDa. Therefore, to provide better resolution, resulting peptide fragments were separated on a large (200 mm) 16.5% Tricine/SDS polyacrylamide gel. The peptides were then transferred from unfixed gel onto PVDF membrane and detected with Coomassie.

As shown in Figure 4, lane 1, four major peptide bands were visualized. Two lower bands of about 7 and 9 kDa have sharp and well-defined boundaries. In contrast, two upper bands with mobilities of 22 and 17 kDa were rather broad and slightly diffuse, typical for peptides containing carbohydrate chains. The results of N-terminal sequence analysis of CNBr peptides from bands 1-4 are shown in Table 2.

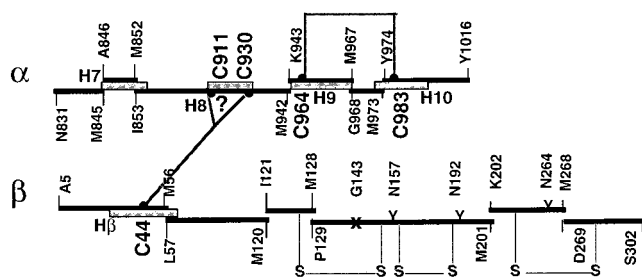


FIGURE 3: Schematic map of the structure of the intersubunit cross-linked product. Locations of the CNBr fragments derived from the C-terminal 22-kDa  $\alpha$ -fragment and  $\beta$ -subunit are marked by N- and C-terminal residues. TM segments H7–H10 and H $\beta$  are shown as filled rectangles. Cu<sup>2+</sup>-phenanthroline-induced disulfide cross-links: intersubunit between Cys44 of H $\beta$  and either Cys911 or Cys930 of H8  $\alpha$  and intrasubunit disulfide bridge between Cys964 (H9) and Cys983 (H10) are shown by wide gray lines. The inner endogenous disulfide bonds of the  $\beta$ -subunit between Cys125–Cys148, Cys158–Cys174, Cys212–Cys275 are indicated as (–S–S–). Residues N157, N192, and N264 indicate N-glycosylation sites. G143 marks the point of partial tryptic cleavage of  $\beta$ -subunit at R142–G143.

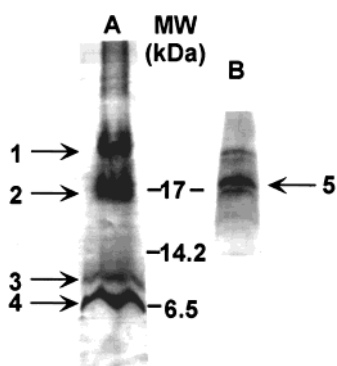


FIGURE 4: Electrophoretic separation of the CNBr fragments of the intersubunit cross-linked product "Bs". Cyanogen bromide cleavage of the intersubunit cross-linked product "Bs" before (lane A) and after deglycosylation with N-glycosidase F (lane B) was done as described in Experimental Procedures. The resulting peptide fragments were resolved on 16.5% Tricine/SDS polyacrylamide gels, transferred onto PVDF membrane, and stained with Coomassie. In experiments with the deglycosylated sample, only part of the gel containing peptide bands of 12–25 kDa were transferred onto PVDF membrane. Peptide bands marked 1 to 5 were excised from the membrane and subjected to N-terminal sequencing. (Results are presented in Table 2.)

On the basis of known primary structure of the dog Na,K-ATPase (41, 42), three sequences, all derived from the  $\beta$ -subunit, were identified in band 1. They represent two consecutive regions of the polypeptide chain: the short octapeptide Ile121–Met128 and the long Pro129–Met201 fragment (see scheme in Figure 3). The latter region contains the trypsin-sensitive bond Arg142–Gly143, which was partially cleaved upon the preparation of Na,K-ATPase membrane moiety (7, 32–34, 36). Thus, the third identified sequence corresponds to the Gly143–Met201 fragment. All these three fragments of the  $\beta$ -subunit remain covalently bound by the native endogenous disulfide bridge Cys125–Cys148. The second inner disulfide bridge connects Cys158 and Cys174. As estimated from the sequence data (Table 2), the N-terminal fragment, Ile121–Met128, is in equimolar stoichiometry with the sum of C-terminal peptides, Pro129–Met201 and Gly143–Met201. Thus, the total molecular mass of the protein moiety of the CNBr peptide fragments present

in band 1 is 7.7–9.3 kDa. The electrophoretic mobility of band 1 corresponds to an apparent molecular mass of ~22 kDa (Figure 4, lane 1), due to the presence of two carbohydrate chains at Asn157 and Asn192 (Figure 3).

We suspected that the rather broad and slightly diffuse band 2 of about 17 kDa may contain more than one product of CNBr cleavage. These might be not only the glycosylated peptide of the  $\beta$ -subunit but also the  $\alpha$ , $\beta$ -cross-linked product, which may be about 17 kDa as mentioned above. Therefore, this band was divided into three portions, and the central part containing the major amount of the peptide material was sequenced first. Two sequences in practically equimolar ratio were identified in band 2 (Figure 3 and Figure 4, lane 1; Table 2). These data indicated that this part of band 2 contains two CNBr peptides originating from two consecutive regions of the C-terminal domain of the  $\beta$ -subunit, Lys202–Met268 and Asp269–Ser302, which remain covalently bound after CNBr cleavage by the endogenous disulfide bridge Cys212–Cys275. This product contains a carbohydrate chain at Asn264; therefore, its electrophoretic mobility is less than expected from the molecular mass of the protein moiety (11.8 kDa).

The only amino acid sequence identified in band 4 corresponds to the CNBr peptide fragment of the  $\beta$ -subunit Leu57–Met120. Its apparent molecular weight is very close to the calculated weight of 7.6 kDa.

N-terminal sequencing of band 3 revealed the presence of two consecutive CNBr peptides from C-terminal domain of the  $\alpha$ -subunit (Figure 3 and Figure 4, lane 1; Table 2). One peptide (Lys943–Met973) represents the major portion of the TM segment H9, containing the single Cys964. The second peptide (Tyr974–Tyr1016) includes the TM segment H10 with the single Cys983. The electrophoretic mobility of band 3 corresponds to the combined molecular mass of the identified peptides it is composed of (8.2 kDa). The peptides are present in equimolar ratio. These data clearly demonstrate that oxidative cross-linking induces a disulfide bridge between Cys964 (H9) and Cys983 (H10) of  $\alpha$ -subunit. The formation of this intrasubunit cross-linked product indicates a close spatial proximity of these Cys residues.

The above sequencing did not reveal the presence of intersubunit cross-linked product but allowed the prediction of the composition of the missing CNBr product: the Cys 44-containing  $\beta$ -fragment (Ala5–Met56) and the  $\alpha$ -fragment (Ile853–Met942), containing Cys911 and Cys930 from H8. The total molecular mass of this cross-linked product is 17.1 kDa. The presence of this product was detected upon sequencing of the upper part of band 2, where it was in a mixture with glycosylated  $\beta$ -fragments (data not shown).

To isolate the desired product, the second large-scale experiment was performed, in which the sample of intersubunit cross-linked product "Bs" (Figure 1, lane 3) was deglycosylated prior to CNBr cleavage. Separation of the resulting peptides was performed as in the first experiment. As shown in Figure 4, lane 2, observed resolution of peptide bands in the 17 kDa zone was significantly improved due to changes of the electrophoretic mobility of glycopeptides after treatment with N-glycosidase F. The strongest and the most clearly defined peptide band 5 with a mobility of about 17 kDa was subjected to N-terminal sequence analysis. As shown in Table 2, two sequences were revealed in equimolar ratio, indicating that the 17-kDa product is composed of an

Table 2: N-terminal Sequences of Isolated CNBr Fragments of the Cross-linked Product Bs<sup>a</sup>

peptide band	apparent $M_r$ (kDa)	sequence	polypeptide chain region	peptide moiety mol mass (kDa)	yield pmol
1	22	<sup>122</sup> Ile-Phe-Glu-Asp-Xaa-Gly	$\beta$ -subunit, Ile121-Met128	0.9	54
		<sup>129</sup> Pro-Ser-Glu-Ile-Lys-Glu	$\beta$ -subunit, Pro129-Met201	8.4	30
		<sup>143</sup> Gly-Glu-Arg-Lys-Val-Xaa	$\beta$ -subunit, Gly143-Met201	6.8	19
2	17	<sup>202</sup> Lys-Tyr-Ser/Asn <sup>b</sup> -Pro-Tyr-Val	$\beta$ -subunit, Lys202-Met267	7.7	68
		<sup>268</sup> Asp-Thr-Glu-Ile-Arg-Ile	$\beta$ -subunit, Asp268-Ser302	4.1	58
3	9	<sup>943</sup> Lys-Asn-Lys-Ile-Leu-Ile	$\alpha$ -subunit, H9, Lys943-Met967	2.8	29
		<sup>968</sup> Tyr-Pro-Leu-Lys-Pro-Thr	$\alpha$ -subunit, H10, Tyr974-Tyr1016	5.4	24
4	7	<sup>57</sup> Leu-Leu-Thr-Ile-Ser-Ser	$\beta$ -subunit, Leu57-Met120	7.6	45
5	17.5	<sup>853</sup> Ile-Gln-Ala-Leu-Gly-Gly-Phe-Phe	$\alpha$ -subunit, H7-H8 Ile853-Met942	10.6	22
		<sup>5</sup> Ala-Lys-Glu-Glu-Gly-Ser-Xaa-Lys	$\beta$ -subunit, Ala5-Met56	6.5	24

<sup>a</sup> The peptide bands marked 1–5 in Figure 3 were analyzed as indicated in Experimental Procedures and in the legend to Table 1. The approximate yield of each sequence was estimated from the average elevation of amino acid residues in cycles 2 through 6 or 8. These values are shown only to illustrate ratios between the components of a particular band. Yield of sequences present in different bands cannot be compared because different portions of each particular band have been sequenced. <sup>b</sup> Practically equal mixture of Asn and Ser was identified on fourth cycle of Edman degradation. There is a Ser residue in this position in the published structure of dog  $\beta_1$ -subunit (41), while  $\beta$ -subunits from other species contain Asn at this position (4). Our data indicate variability of this position in Na,K-ATPase  $\beta$ -subunits from kidneys of different canine strains supplied.

Ile853–Met942  $\alpha$ -fragment of 10.6 kDa and an Ala5–Met56  $\beta$ -fragment of 6.5 kDa. Thus, the isolated peptide is a product of oxidative cross-linking reactions that induced an intersubunit disulfide bridge between Cys44 of H $\beta$  and either Cys911 or Cys930, located in H8 of  $\alpha$ -subunit (Figure 3). The data obtained provide the first direct experimental evidence of the juxtaposition of H $\beta$  and H8 within Na,K-ATPase membrane moiety, indicating that the H8  $\alpha$ -segment is an essential element of intramembrane docking site for the  $\beta$ -subunit. To date, due to insufficient amount of the 17-kDa cross-linked peptide available, we have been unable to perform its further chemical or proteolytic fragmentation needed to determine which particular Cys residue of H8 forms the intersubunit cross-link with Cys44 of  $\beta$ -subunit.

In the above two experiments, practically all the expected CNBr fragments of cross-linked product “Bs”, with the exception of three small  $\alpha$ -fragments (N831–M845, Ala846–Met852, and Gly968–Met973), were isolated and identified by N-terminal sequencing. No products of incomplete CNBr cleavage were detected. These results have demonstrated that CNBr cleavage is a more efficient approach to the fragmentation of hydrophobic polypeptides than proteolytic digestion. Finally, no cross-linked products that might be considered as products of random collisions (random unspecific Cys–Cys interactions) were detected. These observations confirmed that our approach based on solubilization with digitonin preserved the integrity of Na,K-ATPase membrane moiety and that the identified cross-links represent specific native helix–helix interactions between pairs of TM segments H8–H $\beta$  and H9–H10.

**Implication for Spatial Arrangement of the Membrane Domains.** The main result of this study is the direct demonstration that the H8  $\alpha$ -segment is an essential element of intramembrane docking site for the  $\beta$ -subunit. The distances between  $\alpha$  carbon atoms of the half-cystines forming the disulfide bridges in proteins with high-resolution structure range from 3.84 to 6.8 Å (43, 44). Thus, formation of the intersubunit disulfide bridge indicates a close spatial proximity of particular residues (Cys44 of  $\beta$  and Cys911 or Cys930 of  $\alpha$ ) and the tight intramembrane contacts between the corresponding TM segments, H $\beta$  and H8 of  $\alpha$ . Detection of the second induced cross-link between Cys964 and Cys983 of the  $\alpha$ -subunit defines the mutual orientation of H9 and H10 TM helices.

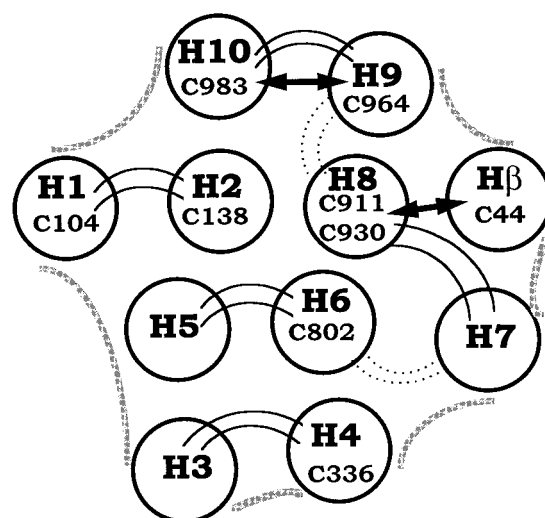


FIGURE 5: Proposed scheme of the packing of the transmembrane segments in the Na,K-ATPase membrane moiety. Contours of the model proposed for SR Ca-ATPase (20) were used as a framework. Scheme represents extracellular view of the TM segments of  $\alpha$ - and  $\beta$ -subunits arranged to accommodate results from this study and other currently available data (See text for details). Intramembrane cysteines are indicated. Solid double lines represent extracellular connecting loops, and dotted double lines correspond to short cytoplasmic loops. Direct helix–helix contacts determined in this study are marked by arrows.

The experimental results from this study and other currently available data are used to propose the updated version of the scheme of the packing of the TM segments in the Na,K-ATPase membrane moiety (Figure 5). Contours of the model proposed for SR Ca-ATPase (23) are used as a framework. As in previous model construction (14, 19–22), we assume that TM segments of  $\alpha$ -subunit linked by short extracellular loops (i.e., H1 and H2, H3 and H4, H5 and H6, and H9 and H10) are associated in pairs forming hairpin structures. Cytoplasmic connection between H8 and H9 is also short enough to consider these TM segments as associated in pair. Therefore, H10, H9, and H8 are shown on the scheme as a chain of contacting TM segments.

Our earlier experiments on the topography of the intramembrane moiety by photolabeling with TID demonstrated that most, but not all, of the TM segments of  $\alpha$ -subunit (H1 and/or H2, H3 and/or H4, H5 and/or H6, as

well as H7, H9, and H10, but not H8) are accessible to the hydrophobic reagent and, therefore, are in direct contact with the lipid bilayer (14, 17, 18). This indicates that H8 TM  $\alpha$ -segment is located in the central part of membrane moiety and encircled by other TM helices, one of which is the TM helix of the  $\beta$ -subunit.

The TM helix of  $\beta$  is placed on the periphery of the  $\alpha\beta$ -complex based on the hydrophobic photolabeling data. Identification of the TID labeled residues within the sequence of  $\beta$ -subunit have demonstrated that about one-third to one-half of its surface is exposed to the lipid bilayer (14, 17, 18). This in turn suggests that at least two, but most likely three, TM  $\alpha$ -segments are involved in the formation of the intramembrane docking site for the TM  $\beta$ -helix. We assume that H7 is a second component of the docking site because results obtained in experiments with mutant constructs showed that the truncated Na,K-ATPase  $\alpha$ -subunit containing TM segments H1–H8 can permanently associate with the  $\beta$ -subunit and form a stable complex (9). Currently, direct interactions between the C-terminal end of the extracellular H7–H8 loop and the  $\beta$ -ectodomain are considered as a key step in  $\alpha\beta$  assembly (5, 6, 8–11). This also argues in favor of H7 placement in close proximity with H $\beta$  and H8.

H1–H2 hairpin is placed as shown because the close spatial proximity between Cys964–Cys983 determined in this study argue that tight interaction of H8 with either H1 or more probably H2 is responsible for formation of 11,22 cross-linked product (7, 22, 23).

Recently, we have made another set of cross-linking experiments that revealed the formation of an intrasubunit disulfide bridge between Cys 802 and either Cys911 or Cys930, indicating that there is a direct interaction between H8 and H6 TM segments (Ivanov, A., and Modyanov N., manuscript in preparation).

Three TM segments (H4, H5, and H6) are placed together because a number of amino acid residues with oxygen-containing side chains were identified in these segments by site-directed mutagenesis and chemical modifications as components of a core region for cation binding and occlusion (for review see refs 45 and 46). Direct contact between H4 and H6 TM segments in SR Ca-ATPase was determined by sulfhydryl cross-linking (24). As mentioned above, H3 should be located next to H4. Obviously, this tentative scheme of TM segments disposition within Na,K-ATPase membrane moiety is only one of several possible arrangements.

Thus, analysis of the spatial structure of the digitonin-solubilized Na,K-ATPase membrane moiety using zero-length cross-linking resulted in identification of points of direct contact between several TM helices. Among these, the H8 segment plays an essential role as a bridge between the  $\beta$ -subunit and the N-terminal domain of the  $\alpha$ -subunit. In this regard, we should emphasize that the ability to form disulfide bridges upon  $\text{Cu}^{2+}$  or  $\text{Cu}^{2+}$ -phenanthroline treatment is not a common feature of intrinsic membrane-buried Cys residues of P-type ATPases. For example, when the membrane moiety of wild-type SR Ca-ATPase, containing seven Cys residues, was treated with  $\text{Cu}^{2+}$ -phenanthroline, no cross-links between intramembrane Cys-residues were detected (Zhao, H., Møller, J. V., and Modyanov, N., unpublished observations).

Finally, it should be noted that the level of structural homology between distinct Na,K- and H,K-ATPases implies

a high degree of similarity in their spatial intramembrane structure. Therefore, we anticipate that data on the arrangement of the Na,K-ATPase TM segments determined in this study are applicable to all X,K-ATPases.

## ACKNOWLEDGMENT

We thank Dr. Amir Askari for helpful discussions and valuable comments on the manuscript and Mano Tillekeratne for excellent assistance.

## REFERENCES

- Horisberger, J.-D. (1994) in *The Na, K-ATPase: Structure-Function Relationship*, pp 1–107, R. G. Landes Company, Austin, TX.
- Møller, J. V., Juul, B., and Le Maire, M. (1996) *Biochim. Biophys. Acta* 1286, 1–51.
- Geering, K. (1992) *Acta Physiol. Scand.* 146, 177–181; (1991) *FEBS Lett.* 285, 189–193.
- Chow, D. C., and Forte, J. G. (1995) *J. Exp. Biol.* 198, 1–17.
- Lemas, M. V., Hamrick, M., Takeyasu, K., and Fambrough, D. M. (1994) *J. Biol. Chem.* 269, 8255–8259.
- Colonna, T. E., Huynh, L., and Fambrough, D. M. (1997) *J. Biol. Chem.* 272, 12366–12372.
- Sarvazyan, N. A., Modyanov, N. N., and Askari, A. (1995) *J. Biol. Chem.* 270, 26528–26532.
- Geering, K., Beggah, A., Good, P., Girardet, S., Roy, S., Schaer, D., and Jaunin, P. (1996) *J. Cell. Biol.* 133, 1193–1204.
- Béguin, P., Hasler, U., Beggah, A., Horisberger, J.-D., and Geering, K. (1998) *J. Biol. Chem.* 273, 24921–24931.
- Hasler, U., Wang, X., Crambert, G., Béguin, P., Jaisser, F., Horisberger, J. D., and Geering, K. (1998) *J. Biol. Chem.* 273, 30826–30835.
- Wang, S.-G. and Farley, R. A. (1998) *J. Biol. Chem.* 273, 29400–29405.
- Jaunin, P., Jaisser, F., Beggah, A. T., Takeyasu, K., Mangeat, P., Rossier, B. C., Horisberger, J. D., and Geering, K. (1993) *J. Cell. Biol.* 123, 1751–1759.
- Eakle, K. A., Kabalin, M. A., Wang, S. G., and Farley, R. A. (1994) *J. Biol. Chem.* 269, 6550–6557.
- Modyanov, N., Lutsenko, S., Chertova, E., and Efremov, R. (1991) *Soc. Gen. Physiol. Ser.* 46, 99–115.
- Ovchinnikov, Y. A., Arystarkhova, E. A., Arzamazova, N. M., Dzhandzhugazyan, K. N., Efremov, R. G., Nabiev, I. R., and Modyanov, N. N. (1988) *FEBS Lett.* 227, 235–239.
- Ovchinnikov, Y. A., Demin, V. V., Barnakov, A. N., Kuzin, A. P., Lunev, A. V., Modyanov, N. N., and Dzhandzhugazyan, K. N. (1985) *FEBS Lett.* 190, 73–76.
- Chertova, E. N., Lutsenko, S. V., Levina, N. B., and Modyanov, N. N. (1989) *FEBS Lett.* 254, 13–16.
- Chertova, E. N., Lutsenko, S. V., and Modyanov, N. N. (1991) *Biol. Membr.* 8, 117–127.
- Efremov, R. G., Gulyaev, D. I., Vergoten, G., and Modyanov, N. N. (1992) *J. Protein Chem.* 11, 665–675.
- Efremov, R. G., Gulyaev, D. I., and Modyanov, N. N. (1992) *J. Protein Chem.* 11, 699–708.
- Efremov, R. G., Gulyaev, D. I., and Modyanov, N. N. (1993) *J. Protein Chem.* 12, 143–152.
- Modyanov, N. N., Vladimirova, N. M., Gulyaev, D. I., and Efremov, R. G. (1992) *Ann. N. Y. Acad. Sci.* 671, 134–146.
- Zhang, P., Toyashima, C., Yonekura, K., Green, N. M., and Stokes, D. L. (1998) *Nature* 329, 835–839.
- Rice, W. J., Green, N. M., and MacLennan, D. H. (1997) *J. Biol. Chem.* 272, 31412–31419.
- Liang, S.-M., Winter, C. G. (1977) *J. Biol. Chem.* 252, 8278–8284.
- Craig, W. S., and Kyte, J. (1980) *J. Biol. Chem.* 255, 6262–6269.
- Periyasamy, S. M., Huang, W.-H., and Askari, A. (1983) *J. Biol. Chem.* 258, 9878–9885.
- Askari, A. (1987) *J. Bioenerg. Biomembr.* 19, 359–374.

29. Giotta, G. J. (1976) *Biochem. Biophys. Res. Commun.* 71, 776–782.
30. Huang, W.-H., Askari, A. (1979) *Biochim. Biophys. Acta* 578, 547–552.
31. Craig, W. S. (1982) *Biochemistry* 21, 5707–5717.
32. Sarvazyan, N. A., Ivanov, A., Modyanov, N. N., and Askari, A. (1997) *J. Biol. Chem.* 272, 7855–7858.
33. Ivanov, A., Askari, A., and Modyanov, N. N. (1997) *FEBS Lett.* 420, 107–111.
34. Or, E., Goldshleger, R., and Karlsh, S. J. (1999) *J. Biol. Chem.* 274, 2802–2809.
35. Ivanov, A. V., Zhao, H., and Modyanov, N. N. (2000) *Biophys. J.* 78, 77A.
36. Capasso, J. M., Hoving, S., Tal, D. M., Goldshleger, R., and Karlsh, J. D. (1992) *J. Biol. Chem.* 267, 1150–1158.
37. Periyasamy, S. M., Huang, W.-H., and Askari, A. (1983) *J. Biol. Chem.* 258, 9878–9885.
38. Schägger, H., and von Jagow, G. (1987) *Anal. Biochem.* 166, 368–379.
39. Vladimirova, N. M., Potapenko, N. A., Sachs, G., and Modyanov, N. N. (1995) *Biochim. Biophys. Acta* 1233, 175–184.
40. Liu, L., and Askari, A. (1997) *J. Biol. Chem.* 272, 14380–14386.
41. Xie, Z., Li, H., Wang, Y., Askari, A., and Mercer, R. W. (1994) in *The Sodium Pump* (Bamberg, E., and Schoner, W., Eds.) pp 49–52, Steinkopff, Germany.
42. Brown, T. A., Horowitz, B., Miller, R. P., McDonough, A. A., and Farley, R. A. (1987) *Biochim. Biophys. Acta* 912, 244–253.
43. Srinivasan, N., Sowdhamini, R., Ramakrishnan, C., and Balaram, P., (1990) *Int. J. Pept. Protein Res.* 36, 147–155.
44. Thornton, J. M. (1981) *J. Mol. Biol.* 151, 261–287.
45. Kaplan, J. H., Gatto, C., Holden, J. P., and Thornewell, S. J. (1998) *Acta Physiol. Scand.* 163 Suppl. 643, 99–105.
46. Lingrel, J. B., Croyle, M. L., Woo, A. L., and Argüello, J. M. (1998) *Acta Physiol. Scand.* 163 Suppl. 643, 69–77.

BI001004J